

# Soft Matter

Accepted Manuscript



This is an *Accepted Manuscript*, which has been through the Royal Society of Chemistry peer review process and has been accepted for publication.

*Accepted Manuscripts* are published online shortly after acceptance, before technical editing, formatting and proof reading. Using this free service, authors can make their results available to the community, in citable form, before we publish the edited article. We will replace this *Accepted Manuscript* with the edited and formatted *Advance Article* as soon as it is available.

You can find more information about *Accepted Manuscripts* in the [Information for Authors](#).

Please note that technical editing may introduce minor changes to the text and/or graphics, which may alter content. The journal's standard [Terms & Conditions](#) and the [Ethical guidelines](#) still apply. In no event shall the Royal Society of Chemistry be held responsible for any errors or omissions in this *Accepted Manuscript* or any consequences arising from the use of any information it contains.

## ARTICLE

## Folic acid/polydopamine nanofibers show enhanced ordered-stacking via $\pi$ - $\pi$ interaction

Cite this: DOI: 10.1039/x0xx00000x

Hailong Fan,<sup>a</sup> Xiang Yu,<sup>a</sup> Yang Liu,<sup>b</sup> Zujin Shi,<sup>b</sup> Huihui Liu,<sup>c</sup> Zongxiu Nie,<sup>c,d</sup> Decheng Wu,<sup>c</sup> and Zhaoxia Jin<sup>a,\*</sup>Received 00th January 2012,  
Accepted 00th January 2012

DOI: 10.1039/x0xx00000x

www.rsc.org/

Recent researches indicate that polydopamine and synthetic eumelanins are optoelectronic biomaterials, in which the one-dimensional aggregate composed of ordered-stacking oligomers has been proposed as unique organic semiconductors. However, improving the ordered-stacking of oligomers in polydopamine nanostructures is a big challenge. Here we first demonstrated how folic acid molecules influence the morphology and nanostructure of polydopamine via tuning  $\pi$ - $\pi$  interactions of oligomers. MALDI-TOF mass spectrometry reveals that porphyrin-like tetramer is characteristic of folic acid/polydopamine (FA/PDA) nanofibers. X-ray diffraction combined with simulation studies indicates that these oligomers favour to aggregate into graphite-like ordered nanostructure via strong  $\pi$ - $\pi$  interaction. High-resolution TEM characterizations of carbonized FA/PDA hybrids show that in FA/PDA nanofibers the size of graphite-like domains is over 100 nm. The addition of folic acid in polydopamine enhances the ordered stacking of oligomers in its nanostructure. Our study steps forward to discover the mystery of the structure-property relationship of FA/PDA hybrids. It paves a way to optimize properties of PDA through designing and selecting oligomer structure.

### 1 Introduction

In 1981, Waite and Tanzer reported that the adhesive discs of marine mussel are rich in the catecholic amino acid 3,4-dihydroxyphenylamine (DOPA) and they indicated further that the composition of mussel protein attributes to byssal adhesion.<sup>1</sup> After over thirty years, mussel-inspired surface chemistry has great progress recently. Natural and synthetic adhesives composed of DOPA and its derivatives attract great attention for their strong interfacial adhesion strength.<sup>2-6</sup> Adhesive proteins of mussels inspire a versatile approach to the surface modification for a wide range of inorganic and organic materials,<sup>7-9</sup> leading to multifunctional coating for a variety of applications.<sup>10,11</sup> Particularly, polydopamine (PDA) coating shows great applications in biomedical applications.<sup>10,12</sup> It not only provides a stable media to bind a wide variety of biomolecules, but also changes biocompatibility of materials to increase cellular adhesion and proliferation.<sup>13</sup> There are also reports of their applications in biological analysis and blood transfusion.<sup>14,15</sup> Many studies presented that multipurpose surface modification of various substrates can be simplified to a one-pot protocol in which different substrates are immersed in a solution containing dopamine and other targeting agents.<sup>5,16-20</sup> The existing of different molecules has rarely shown influences to the self-polymerization of dopamine. However, our previous study presented that folic acid (FA), a small molecule with multiple biofunctions, can dramatically influence the morphology of polydopamine, leading to the formation of FA/PDA nanofibers under a particular experimental

condition.<sup>21</sup> Because only a few molecules, folic acid and tris-buffer, are observed to show ability to manipulate self-polymerized nanostructures of dopamine till now,<sup>21,22</sup> revealing their roles in the generation of polydopamine will help us understand the reaction mechanism deeply.

Moreover, the oxidation and self-polymerization of dopamine not only leads to surface modification, but also results in polydopamine nanoparticles, which are insoluble and highly aggregative nanoparticles that are synthetic analogue of the naturally occurring melanin.<sup>23-28</sup> Melanin is an important biopolymer which can protect humans from the ultraviolet injury, remove free radical and participate in nervous system activities.<sup>29,30</sup> Ju et al. demonstrated that melanin-like polydopamine nanoparticles possess free radical scavenging activity.<sup>25</sup> Recently, Liu et al. demonstrated that dopamine-melanin nanospheres synthesized by the oxidation and self-polymerization of dopamine are efficient near-infrared photothermal therapeutic agent for cancer therapy.<sup>31</sup> Folic acid, a water soluble vitamin of the B-complex group, known as an effective therapy in the prevention of birth defects.<sup>32</sup> Recent research revealed that because cancer cells have a larger need of folic acid to synthesize nucleotide bases in cell proliferation, they show over-expression of folate-receptors. So folate-modification is often used to increase the uptake of anti-cancer drugs by tumors, and folate-modified nanoparticle drug delivery systems have demonstrated an improved efficacy in delivering hydrophobic drugs.<sup>33</sup> If folic acid is immobilized in polydopamine nanoparticles, the near-infrared photothermal therapeutic agent can be better target-delivered to tumor.

FA/PDA hybrids will be a potential candidate of drug-deliver for cancer therapy. Therefore, the detailed study of FA/PDA nanostructure is not only important to discover the formation mystery of different FA/PDA nanostructures, but also beneficial to their biomedical applications in future.

Matrix-assisted laser/desorption ionization (MALDI) mass spectrometry is a powerful tool to elucidate the composition and polymerization mode of melanins and polydopamine. Most of mass spectrometry characterizations of melanins show peaks at lower mass units (usually less than 1500 Da), suggesting an oligomer-aggregated (mainly, tetramer, pentamer or hexamer) nanostructure of melanins.<sup>34-37</sup> It also suggests a stepwise pattern of melanins formation. The mass distribution of melanins consists with the chemical disorder model proposed based on studies of optical property of melanins.<sup>38,39</sup> Herein we investigated the structural features of FA/PDA nanostructures in molecular level through detailed MALDI-TOF MS characterizations. MALDI-TOF MS characterizations of FA/PDA nanostructures, both nanoparticles and nanofibers, present plentiful information of chemical structures of hybrids. Combining with characterizations and simulation results, we identified possible oligomers existing in FA/PDA nanostructures, especially the porphyrin-like tetramers in FA/PDA nanofibers. This study shows that the addition of folic acid in the self-polymerization of dopamine will modulate oligomers' structure, which further influences the morphology of FA/PDA nanostructures. HRTEM characterization of carbonized FA/PDA nanofibers observed extraordinary large domains of graphite-like nanostructures, indicating an increase of ordered-stacking through  $\pi$ - $\pi$  interaction that is also coincident with XRD measurements. Moreover, zeta potential, fluorescence and free-radical scavenging activity of FA/PDA nanoparticles were measured and compared with pure PDA nanoparticles. This study helps us to understand how folic acid modulates dopamine polymerization in nanostructures and their properties.

## 2 Experimental sections

### 2.1 Materials.

Dopamine hydrochloride (purity 98%) was purchased from Sigma-Aldrich. Tris (hydroxymethyl) aminomethane (tris) - HCl buffer (pH = 8.8) was obtained from Shanghai Double-Helix Biotech. Co. Ltd. Folic acid (FA, purity  $\geq$  97.0%), sodium hydroxide (NaOH) and ascorbic acid (99.7%) were purchased from Sinopharm Chemical Reagent Co. Ltd. 2,2-diphenyl-1-picrylhydrazyl (DPPH, 96%) was purchased from Aladdin company (Shanghai, China). All these reagents are used as received. All solutions were prepared by using Millipore water.

### 2.2 Fabrication of PDA and FA/PDA hybrids.

Polydopamine nanoparticles were synthesized through oxidative-polymerization of dopamine. Typically, dopamine (0.3 mg/mL) was dissolved in tris-HCl buffer solution (10 mM, pH = 8.8). The solution was stirred for 24 hours and oxidation of dopamine was achieved by saturated O<sub>2</sub> in solution. Then the obtained dark suspension was centrifuged at 10,000 rpm for 30 min to collect the sediment. The sediment was washed several times with fresh water to remove un-reacted dopamine, and it was then dried by freeze-drying (-58 °C, 5~6 Pa).

**Route 1:** To prepare large FA/PDA nanoparticles, the concentration of folic acid and dopamine in water is 0.1 and 0.3

mg/mL, respectively. Tris-HCl buffer (10 mM, pH = 8.8) was added to above mixture solution to adjust its pH value. Then the mixed solution was stirred at room temperature for 24 hrs to conduct self-polymerization. The product was collected through centrifugation at 10,000 rpm for 30 min. It was washed by using fresh water several times, and then collected and dried by freeze-drying.

**Route 2:** In a typical experiment, dopamine and folic acid were first dissolved in deionized water and stirred over 1 day (concentration of dopamine ~0.3 mg/mL, concentration of folic acid is varied from 0.1-0.2 mg/mL) at 60 °C in dark, then tris-HCl buffer was added to above solution and let the concentration of tris-HCl be 10 mM (pH = 8.8), and kept stirring for 3 hrs at 60 °C in dark. Although the solubility of folic acid in neutral water is very low, it dissolves very well in weak base tris-HCl buffer solution. The color of mixed solution turns to yellow after the addition of tris-HCl buffer, and with the oxidation and self-polymerization of dopamine, the color changes to brown and finally black. NaOH aqueous solution (0.1 M) was also used to adjust the pH value (pH = 8.3) of mixture solution of dopamine and folic acid and induce self-polymerization of dopamine. FA/PDA nanofibers were also obtained in NaOH case. Then the dark suspension was centrifuged at 10,000 rpm for 30 minutes to collect the obtained hybrid nanofibers. The sediment was washed several times with fresh water and then dried by freeze-drying. Dried powder was used to conduct morphological and chemical characterizations. Clean FA/PDA nanofibers were re-dispersed in water for further use.

To prepare small FA/PDA nanoparticles, the concentration of dopamine is 0.6 mg/mL, the concentration of folic acid is 0.3 mg/mL. The reaction was conducted at 60 °C under dark. The mixture of folic acid and dopamine was stirred for 24 h, then tris-buffer (pH = 8.8, 10 mM) was added in above mixture to adjust its pH value to 8.8. The reaction time was 3 hrs after adding tris-buffer. Finally, the suspension was centrifuged at 10,000 rpm for 30 min to collect product. The sediment was washed several times with fresh water and then dried by freeze-drying.

### 2.3 General characterizations.

PDA or FA/PDA nanocomposites were coated with a thin layer of gold before the characterization using scanning electron microscopy (SEM, JEOL 7401). A drop of PDA nanoparticle suspension in water was placed onto copper grid for transmission electron microscope characterization (Hitachi TEM, H-7650B) with an accelerating voltage of 100 kV. The optical absorption of pale-brown aqueous suspension of PDA nanoparticles was measured by using UV-Vis spectrophotometer (Varian Cary 50). Dried powder of PDA nanoparticles was further characterized by using Fourier Transform Infrared spectrometer (FTIR, Shimadzu Cor. IRPrestige-21). The zeta potential values of FA/PDA nanoparticles (route 2) in aqueous solution at different pH values were measured on a Brookhaven ZetaPALS (Brookhaven Instrument, USA) at 25 °C. Measurements were performed five times for each sample. Steady-state fluorescence spectra were measured on Fluorescence Spectrophotometer (F-4600, Hitachi). For FA, FA/PDA nanofibers, and FA/PDA nanoparticles, the excitation wavelength was set 360 nm. Fluorescence lifetimes were measured by an Edinburgh Instrument LifeSpec Red Spectrometer (laser: 372 nm), all measurements were performed at room temperature.

#### 2.4 DPPH assay for antioxidant activities of PDA, FA/PDA nanoparticles.

The antioxidant activities of PDA, FA/PDA nanoparticles and nanofibers were measured by DPPH assays as described in literature.<sup>25</sup> Fresh DPPH /ethanol (0.1 mM) solution was used in measurements. 180  $\mu$ L of different concentrations of PDA or FA/PDA nanocomposites suspensions was added to 4 mL of DPPH. The tested amount of PDA or FA/PDA nanocomposites was changed from 5 to 240  $\mu$ g. The scavenging activity was evaluated by measuring the absorbance change at 520 nm after tested mixture was kept in the dark for 20 min.

#### 2.5 MALDI-TOF characterizations of PDA nanoparticles, FA/PDA nanoparticles and nanofibers.

$\alpha$ -Cyano-4-hydroxy cinnamic acid (CHCA) 98% purity was purchased from Sigma Aldrich Inc. (St. Louis, MO). HPLC-grade acetonitrile and trifluoroacetic acid (TFA) were purchased from Fisher Scientific (USA). Triple deionized water was prepared from Millipore water purification system (Millipore, Billerica, MA, USA) in our laboratory whenever necessary. The solution of matrix CHCA (10 mg/mL) was prepared in CH<sub>3</sub>CN/water (1:1, v/v) containing 0.1% TFA. 1  $\mu$ L of the analyte was premixed with 1  $\mu$ L of the matrix in a centrifuge tube, and then 1  $\mu$ L of the resulting mixture was pipetted on the MALDI target plate and air-dried for MALDI-TOF MS analysis. MALDI-TOF MS analysis was performed on an Ultraflextreme MALDI-TOF/TOF mass spectrometer (Bruker Daltonics, Billerica, MA) equipped with a Nd:YAG/355 nm Smart Beam TM laser. The laser was operated at 2000 Hz in positive reflectron mode. The mass spectrometer parameters were set as the manufacturer recommended and adjusted for optimal acquisition performance. The laser spot size was set at medium focus (~50  $\mu$ m laser spot diameter). The mass spectra data were acquired over a mass range of  $m/z$  0~3000 Da and each mass spectrum was collected from accumulation of 200 laser shots. Mass calibration was carried out with external standards prior to data acquisition.

#### 2.6 High-resolution TEM characterizations of carbonized FA/PDA hybrids.

FA/PDA nanoparticles and nanofibers were pyrolysed in N<sub>2</sub> at a heating rate of 5  $^{\circ}$ C/min, from room temperature to 750  $^{\circ}$ C and kept at 750  $^{\circ}$ C for 1 hr. The residue of carbonized FA/PDA hybrids was re-dispersed in ethanol via sonication and conducted morphological and structural characterizations. High resolution TEM was conducted by using JEM-2100 (JEOL) at 200 kV.

#### 2.7 Computational Method.

Gaussian 09 package was used to optimize the molecule geometries. The geometry optimizations were performed in the gas phase with density functional theory (DFT) with hybrid functional (B3LYP) and 6-31+G\* basis set.<sup>40</sup> Next, several optimized molecules were collected and input into MOPAC 2012 package to calculate the  $\pi$ - $\pi$  interaction of optimized molecules using the semiempirical PM7 method.<sup>41,42</sup>

### 3 Results and discussion

The fascinating feature of polydopamine as surface modifier is because different targeting agents, such as ATRP initiator, polysaccharide and growth factor, can be successfully immobilized in polydopamine adhesion layer via oxidation and self-polymerization of dopamine.<sup>18</sup> These studies indicate that the existence of these additives in dopamine solution has no significant influence to the oxidation and self-polymerization of dopamine. However, hybrids of polydopamine and folic acid showed difference via one-pot process. Fig. 1a presents experimental scheme of the fabrication of FA/PDA hybrids. In our experiments, we observed that if tris-HCl buffer was immediately added in the mixture of dopamine and folic acid dissolved in water at room temperature, the obtained hybrids nanoparticles have a diameter of over 100 nm, which just look like ordinary PDA nanoparticles (Fig. 1b). We marked this process as Route 1. However, when dopamine and folic acid were dissolved in water and were stirred for over 24 hr in dark at 60  $^{\circ}$ C, and then tris-HCl buffer or NaOH aqueous solution was added to adjust the pH value of mixed solution and triggered the self-polymerization of dopamine, the product is different with that obtained in Route 1. We named this process as Route 2. Depending on the concentration of dopamine and folic acid, FA/PDA nanoparticles and nanofibers are generated in Route 2 (Fig. 1c-e). The diameter of FA/PDA nanoparticles generated through Route 2 is 50~60 nm (Fig. 1c). The most interesting phenomenon is FA/PDA nanofibers generated through Route 2 (Fig. 1d and e). Temperature shows great influence to the morphology of self-polymerized hybrid nanostructures.<sup>21</sup> The temperature range between 45~60  $^{\circ}$ C is optimized temperature window to generate FA/PDA nanofibers in good quality on the basis of our previous study.<sup>21</sup> Bernsmann et al. has indicated that the property of polydopamine depends on the used oxidant and buffer solution.<sup>43</sup> In our case, we have tried two basic solutions to adjust the pH value of reaction solution, tris-HCl buffer (pH = 8.8, 10 mM) or NaOH solution (0.1 M), respectively. We noticed that the nanofibers generated in tris-HCl buffer (Fig. 1d) is cleaner than that in NaOH (Fig. 1e), more nanoparticles mixed in later case. Additional separation step is needed to generate clean nanofibers. Usually simple centrifugation of mixture suspension at lower speed (3000 rpm, 10 min) will condense nanofibers in sediment.

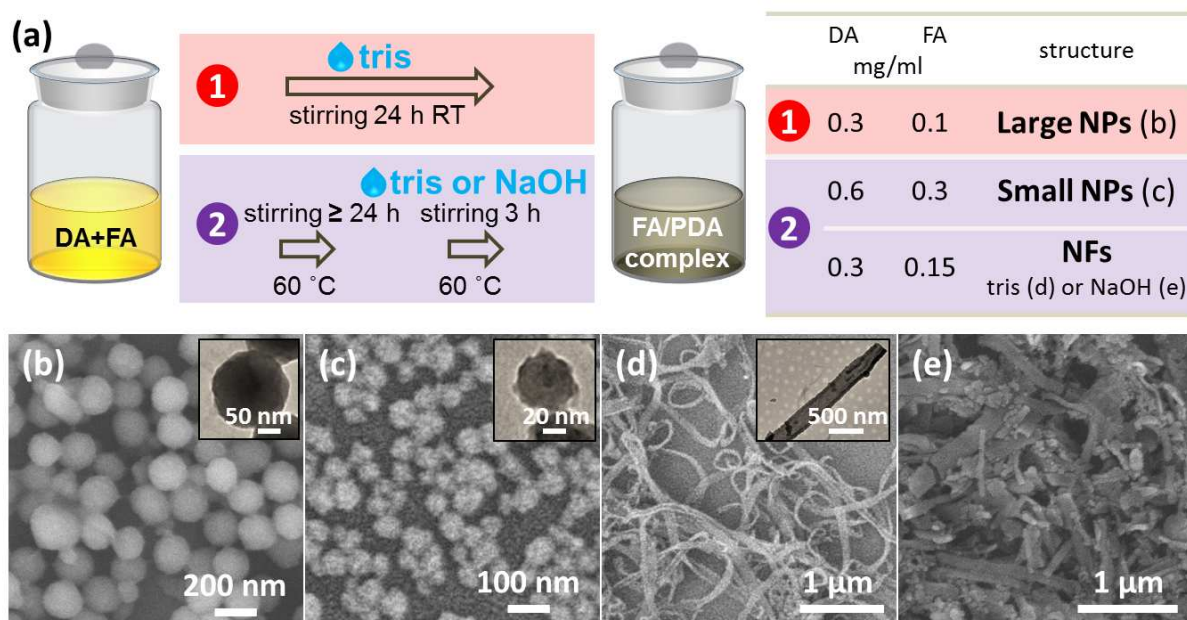


**Fig. 1** (a) Scheme of fabrication procedures of different FA/PDA nanostructures, (b) SEM image of large FA/PDA nanoparticles generated in Route 1, (c) SEM image of small FA/PDA nanoparticles obtained in Route 2, (d, e) SEM images of FA/PDA nanofibers obtained through Route 2: (d) Tris-HCl buffer, 10 mM, pH = 8.8, (e) NaOH aqueous solution, pH = 8.3. The pictures inset in 1b-1d were TEM images of corresponding nanostructures.

Because MALDI mass spectrometry can provide valuable information about FA/PDA compositions, we conducted a comparative study of FA/PDA nanostructures (nanoparticles and nanofibers generated through Route 2) and pure PDA nanoparticles by using MALDI-TOF mass spectrometry. We are hoping to learn deeply about the structure of FA/PDA in molecular level. Fig. 2 presents MALDI mass spectra of four different samples, FA/PDA nanoparticles, FA/PDA nanofibers generated in NaOH or tris-buffer, and pure PDA nanoparticle as contrast. Generally, these four spectra share many similarities: 1) Maximum value of  $m/z$  in four spectra is  $< 1100$ ; 2) The appearance of peaks is in group; 3) The value difference between some adjacent peaks is  $\sim 16$ , which is often observed in melanin's MS characterizations, and it is assigned to leaving of OH.<sup>6,11</sup> Recently, Reale et al. first reported the observation of molecules with higher mass units: more than 5000 mass units for DHI and more than 8000 Da for N-methyl-5,6-dihydroxyindole by using high resolution MALDI, which means oligomeric species composed of more than ten hydroxyindole moieties.<sup>44</sup> We have not observed peaks at higher mass units in FA/PDA hybrids, which may be due to the oxidation process of dopamine in folic acid environment has been disturbed by the self-assembly of folic acid. In addition, the oxidized product of dopamine by  $O_2$  (in our synthesis) may be slightly different from that oxidized by horseradish peroxidase and  $H_2O_2$ .<sup>44</sup> This MALDI data suggest that the molecular constituents of FA/PDA are smaller compared to their nanostructure's size revealed by morphologic characterizations. As a result, it is reasonable to suppose that oligomers aggregate to form FA/PDA nanostructures in micrometer size. Based on  $m/z$  values of four samples and literature results, we conducted assignment for these common peaks showing in all four samples (Fig. S1-S4, Table S1). We tentatively collected them to trimer (III), tetramer (IV), pentamer (V), hexamer (VI) and octamer (VIII). The possible chemical structures of these oligomers are also proposed and showed in Fig. S5. We can confirm that FA/PDA hybrid

nanostructures share chemical similarity with pure PDA, but they have some characteristic structure in molecular level, which is due to the influence of folic acid to the self-polymerization of dopamine.

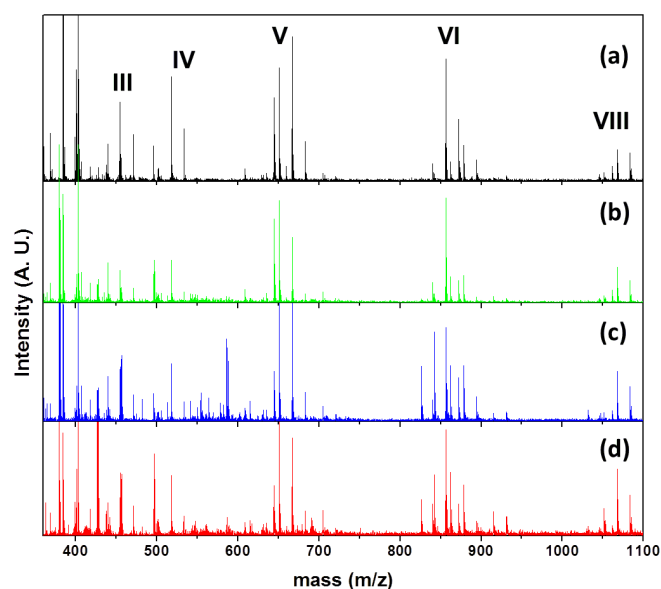


**Fig. 2** MALDI-TOF spectra of (a) PDA nanoparticles, (b) FA/PDA nanoparticles, (c) FA/PDA nanofibers (NaOH), and (d) FA/PDA nanofibers (tris-HCl buffer), respectively.

Compared with these common peaks, we are much more interested in those special peaks showing only in folic acid hybrid samples. We have observed two special features, which appear in folic acid hybrids, especially only in FA/PDA nanofibers. The first one is the  $m/z$  peak of folic acid, which is 440.7 Da, showing in all folic acid hybrid nanostructures (Fig.

S1). The second one is a peak group around 584-589 Da (Fig. 3a) which only exists in FA/PDA nanofibers, and the  $m/z$  value is between that of chain-like tetramers and pentamers (Table S1). Kaxiras et al. have proposed a cyclic tetramer model based on their studies of absorption spectrum of melanins, but this cyclic tetramer has not been observed experimentally before.<sup>45,46</sup> They have listed the basic monomer structures for generating tetramers or pentamers further are hydroquinone (HQ), its redox forms indolequinone (IQ), tautomers quinone-methide (MQ or QI1) and quinon-imine (QI2). We found that the specific peak ( $m/z = 586.001$ ) existing only in MS spectra of FA/PDA nanofibers (Fig. 3a) can be fitted to cyclic tetramer of DHI arranged in QHQH manner very well. It may be assigned to tetramer (QHQH) + H (the molecular weight of QHQH is 584.491 Da) (Fig. 3c). To fit with other MS peaks (587, 588, 589 Da), the tetramer structure requires increase of the number of H which may produce tetramer structures composed of more hydroquinone (HQ). Although other tetramer structures with more hydroquinone may not be the stable structure in the point of view of thermodynamics, they may exist in FA/PDA products due to the selectivity of specific experimental conditions.<sup>45,46</sup> On the other hand, we noticed that Liebscher et al. have reported the appearance of 589.1354 Da in ES(+)-HRMS peaks of PDA samples, although it is only several (3~4) ppm.<sup>47</sup> It is also observed in MALDI-TOF MS spectra of melanochromes generated by enzymatic oxidation (peroxidase/H<sub>2</sub>O<sub>2</sub>) of dopamine in sodium phosphate buffer reported by Kroesche and Peter.<sup>35</sup> All these MS peaks have been assigned to cyclotetramer of DHI.

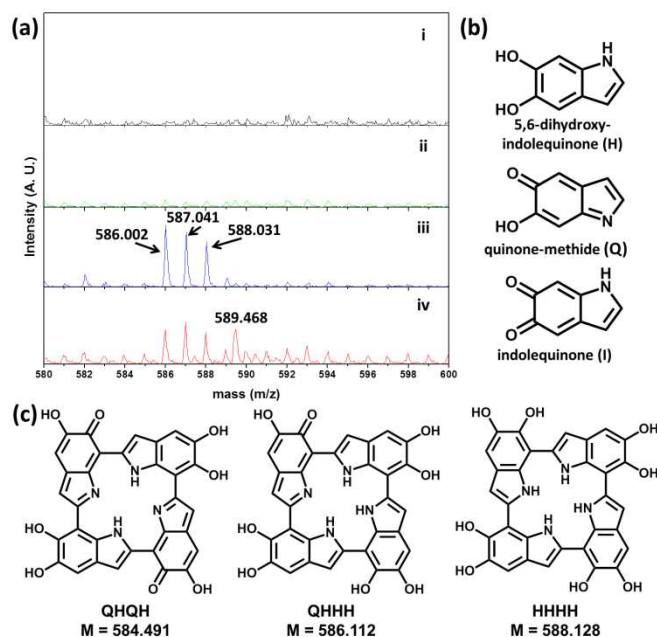


**Fig. 3** (a) Segmental spectrum of MALDI-TOF ( $m/z$ : 580-600) characterizations of PDA nanoparticles (i), FA/PDA nanoparticles (ii), FA/PDA nanofibers (NaOH) (iii), and FA/PDA nanofibers (tris-HCl buffer) (iv), respectively. (b) Chemical structures of 5,6-dihydroxy-indolequinone (H), quinone-methide (Q), and indolequinone (I). (c) Three possible tetramer structures.

In our previous study, we have discussed the similarity of porphyrin-like tetramer of melanins with the self-assembled cyclic complex of folic acid.<sup>21</sup> We hypothesized that the

self-assembled complex of folic acid is involved in the self-polymerization of dopamine, leading to the formation of FA/PDA hybrid nanofibers. These peaks around 584-589 Da only showed in FA/PDA nanofibers, and can be fitted to cyclic tetramer structure very well, which may somehow supports our hypothesis that cyclic tetramer is an important structural motif in FA/PDA nanofibers. We further conducted calculation to investigate the interaction between these cyclic tetramer structures (Fig. 4). Semiempirical PM7 method calculation shows that strong  $\pi$ - $\pi$  interaction existed between oligomers. The distance between these stacking layers are 3.4 Å. The  $\pi$ - $\pi$  interaction between other tetramers is similar with that of QHQH tetramers (Fig. S6). Meredith and Sarna reported that van der Waals and  $\pi$ - $\pi$  interaction between protomolecules contribute mainly to the stacked structure to construct "secondary structures".<sup>39</sup> Powder X-ray diffraction (XRD) has been used to elucidate  $\pi$ - $\pi$  interaction in eumelanins and PDA nanoparticles,<sup>48,49</sup> so we compared XRD characterizations of FA/PDA nanoparticles and nanofibers (Fig. 5). The broad peak ( $2\theta = 23.4^\circ$ ) corresponding to  $\pi$ - $\pi$  stacking structure in polydopamine is stronger in FA/PDA nanofibers than that in FA/PDA nanoparticles.<sup>49</sup> Combining the XRD characterization with abovementioned MALDI-TOF results and DFT calculations, we propose that because of the formation of cyclic tetramer in FA/PDA nanofibers, enhanced  $\pi$ - $\pi$  interaction exists in nanofiber samples. But the relation between the enhanced  $\pi$ - $\pi$  interactions and one-dimensional nanofiber morphology is still unclear. Chen et al. have observed that porphyrin-like tetramers tend to arrange themselves in random-like orientations based on their simulated aggregate made of 375 IMIM tetramers.<sup>50</sup> We suppose that the influence of folic acid to the formation of polydopamine nanofibers is not only favoring the generation of porphyrin-like tetramers, but also something else which can direct the orientation of oligomers. That may need deeper investigations in future. In addition, we noticed that Della Vecchia et al. have reported the remarkable relations of cyclized (indole) and uncyclized (catecholamine) units with starting dopamine concentrations.<sup>14</sup> The proportion of DHI units is higher in the lower starting dopamine concentration (0.5 mM) than those from higher dopamine concentration (10 mM). In the synthesis of FA/PDA nanostructures (Route 2), doubled concentrations of dopamine and folic acid will lead to the generation of small FA/PDA nanoparticles (Fig. 1c), instead of FA/PDA nanofibers produced in lower concentrations. That may also support their opinion that the variation of dopamine concentration influences the structure of oligomers and polymerization pathway.

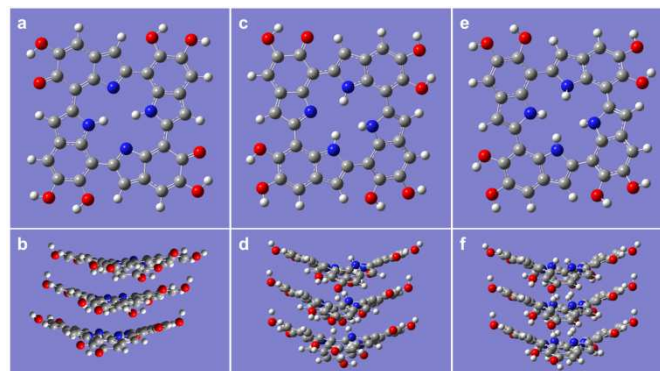


**Fig. 4** Optimized molecule structures and three-layer stacked structures of (a, b) QHQH, (c, d) QHHH, and (e, f) HHHH, respectively. Atom colour: white: H, gray: C, red: O, blue: N.

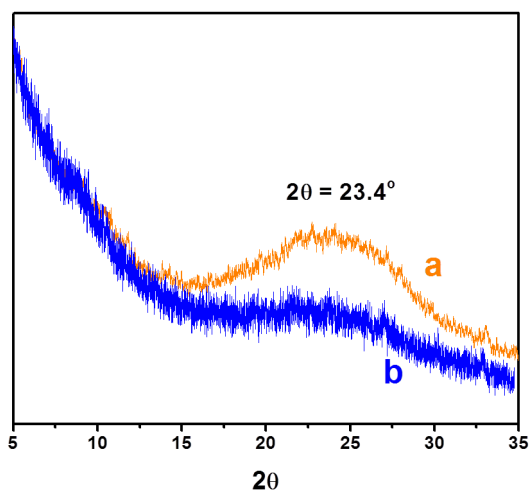


**Fig. 5** X-ray diffraction spectra of FA/PDA (a) nanofibers and (b) nanoparticles (route 2).

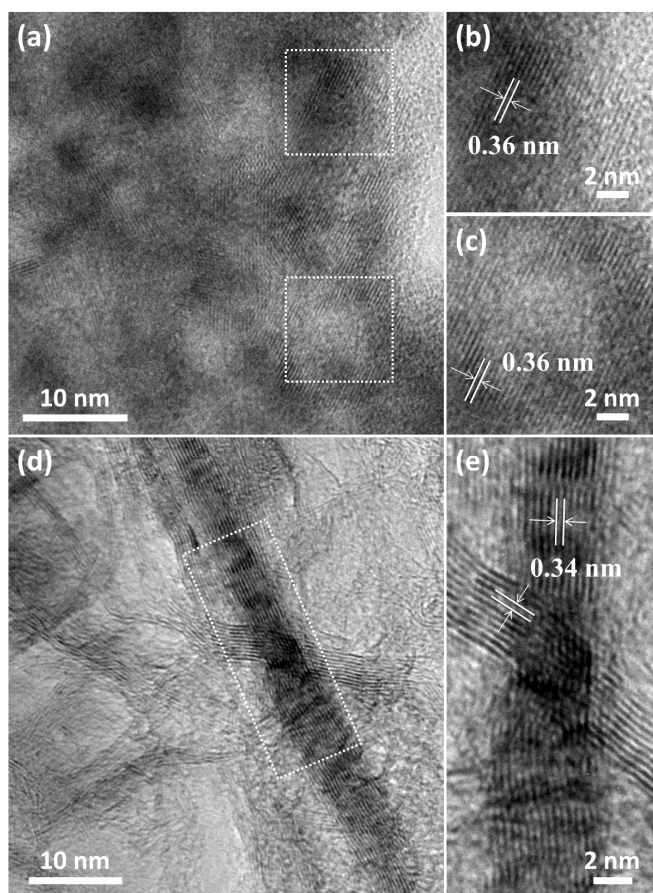


**Fig. 6** HRTEM images of carbonized FA/PDA (a-c) nanoparticles (route 1) and (d, e) nanofibers (tris-HCl). For nanoparticles, the layer distance of graphite-like domains is 0.36 nm. For nanofibers, graphite-like domain has a length of over 100 nanometers. The layer distance is about 0.34 nm.

On the other hand, our previous study has reported that HRTEM characterization of carbonized PDA nanoparticles is a good way to identify ordered nanostructure in PDA.<sup>51</sup> Here we also characterized the carbonized FA/PDA nanostructures

through HRTEM. Fig. 6 is HRTEM images of carbonized FA/PDA nanoparticles (route 1) and nanofibers. Graphite-like domains containing ordered stacking layers are observed in both cases, however, the length of stacking layers in FA/PDA nanofibers is much longer than that observed in FA/PDA nanoparticles, although layer distances are similar in these domains in nanoparticles ( $\sim 0.36$  nm) and nanofibers ( $\sim 0.34$  nm). These HRTEM images further confirmed that the aggregated nanostructure in FA/PDA nanofibers is ordered in a longer range than that in FA/PDA nanoparticles.

The next question needs be answered is the property of FA/PDA hybrid nanostructures. Does folic acid molecule in hybrid nanostructures still behave like free folic acid? Can we still use it to guide the target-delivering of drugs based on PDA nanoparticles? The existing of FA molecules in FA/PDA nanoparticles is confirmed by MALDI-TOF (Fig. S1). But it is hard to know if folic acid conjugates to polydopamine with covalent bond or only mixes with polydopamine keeping its own chemical properties. Previous study reported that large PDA nanospheres (diameter is  $336.0 \pm 37.5$  nm) have fluorescence quenching ability equivalent to that of superquencher, the graphene oxide.<sup>52</sup> As we know that folic acid is a weak fluorescent, but we found that FA/PDA hybrid nanoparticles and nanofibers show similar fluorescence spectrum with folic acid, no clear quenching effect is observed in FA/PDA hybrids (Fig. 7a). Their fluorescence lifetimes are also in similar level (Fig. 7b). Zeta potential of these FA/PDA nanoparticles (route 2) is showed in Fig. 7c. It is observed that surface charge of FA/PDA nanoparticles has been converted from positive to negative at pH value  $\sim 4$ . The surface charge of FA/PDA nanoparticles is below  $-30$  mV at physiological environment that is an advantage for their biomedical applications. Larger FA/PDA nanoparticles have similar surface property. Ju et al. have reported their study of antioxidant activity of melanin-like and surface-modified melanin-like nanoparticles.<sup>25</sup> Compared with their melanin-like nanoparticles which have varied size from  $68 \pm 21$  nm to  $107 \pm 24$  nm, suspensions of FA/PDA nanoparticles have slightly smaller sizes and they show good stability in aqueous solution without any surface modification. We compared the radical scavenging activity of FA/PDA nanoparticle (route 1), FA/PDA nanofibers, pure PDA nanoparticle ( $\sim 100$  nm in diameter) and ascorbic acid (Fig. 7d). DPPH assay is used to measure free radical scavenging activities. The carbon-centered radicals and semi-quinone moiety of PDA nanoparticles are responsible for reducing free radicals.<sup>53,54</sup> The scavenging DPPH-radical effect is dose-dependent for PDA, FA/PDA nanofibers, and FA/PDA nanoparticles. The efficient concentration ( $EC_{50}$ ) value, at which the initial DPPH concentration is decreased by 50%, is often used to compare antioxidant activity.  $EC_{50}$  value of PDA nanoparticles, FA/PDA nanofibers, and FA/PDA nanoparticles are  $23.3 \mu\text{g}$ ,  $22.6 \mu\text{g}$ , and  $36.7 \mu\text{g}$ , respectively. They are slightly lower than that of ascorbic acid (AA), which may be due to the lower efficiency of functional groups inside nanoparticles than that in molecules. And more compact  $\pi$ - $\pi$  stacked oligomers structure will reduce accessibility of free radicals to aggregated nanoparticles.<sup>54</sup> In our further study, a deeper investigation of polymerization mechanism of dopamine and their structural features in multilevel will be conducted. Such a bottom-up study will bridge our knowledge gap between polydopamine chemistry, morphology and functions, leading to elegant control of the properties of polydopamine and its functional hybrids.

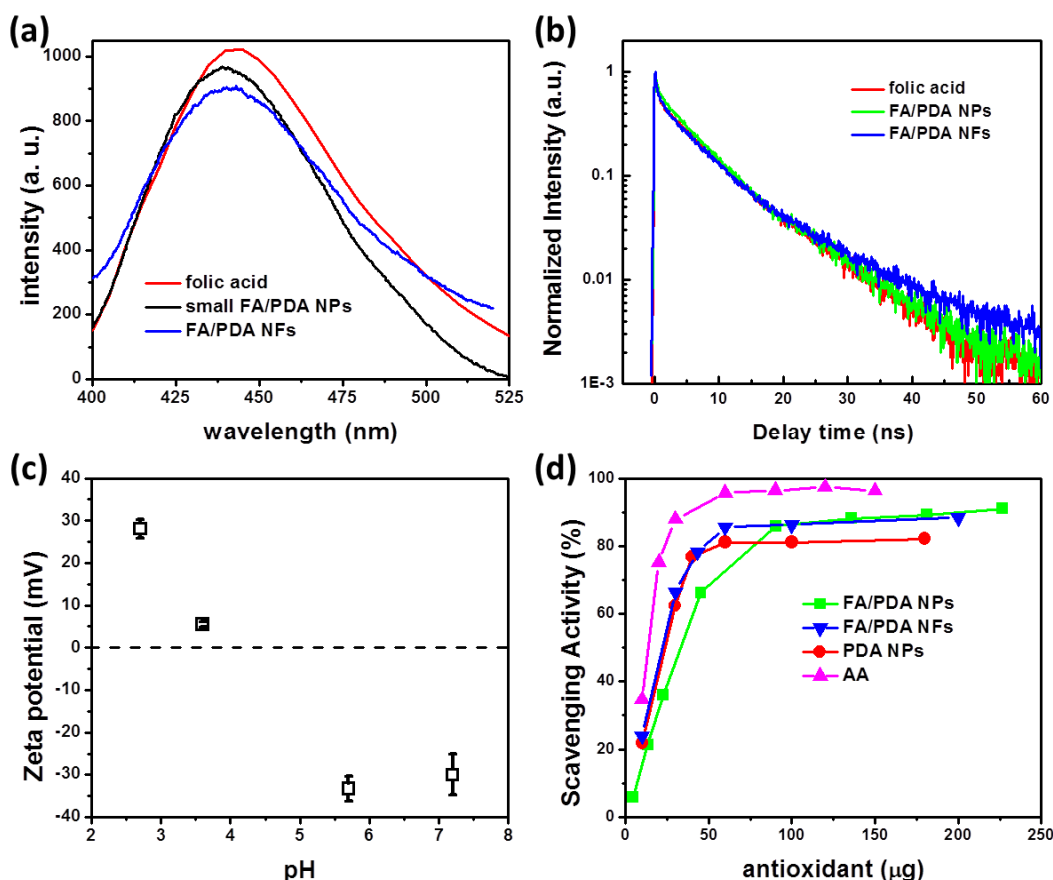


**Fig. 7** (a) Fluorescence spectra of FA (5  $\mu\text{M}$  in water), FA/PDA nanoparticles (4  $\mu\text{g}/\text{mL}$ , route 2), and FA/PDA nanofibers (4.25  $\mu\text{g}/\text{mL}$ ), excitation wavelength is 360 nm. (b) Fluorescence decay curves of folic acid, FA/PDA nanoparticles (route 2), and FA/PDA nanofibers. (c) Zeta potentials of FA/PDA nanoparticles (route 2) in aqueous solution at different pH values, (d) DPPH radical scavenging activity of FA/PDA nanoparticles (route 1), FA/PDA nanofibers, and PDA nanoparticles (route 1) (compared with ascorbic acid).

## Conclusions

In this study, we investigated the influence of folic acid to polydopamine, both in hierarchical structure features and hybrid properties. On the basis of MALDI-TOF MS characterizations, simulation studies and previous literature reports, we tentatively identified the special cyclic tetramer structures in FA/PDA nanofibers. We noticed that strong  $\pi$ - $\pi$  interactions exist between proposed tetramers, which are coincident with our XRD measurements and HRTEM characterizations of carbonized FA/PDA nanostructures. Our study confirmed that the addition of folic acid favors the formation of cyclic tetramers in hybrid nanofibers, causing an enhanced  $\pi$ - $\pi$  interaction in nanofibers. The understanding of structural changes of polydopamine generated in folic acid will help us to fabricate hybrid FA/PDA nanomaterials with controllable properties, which will have promising applications in energy, biomedical and environmental areas.

## Acknowledgements

The authors gratefully acknowledge the National Natural Science Foundation of China (Grants 21374132, 51173201) for financial support. Prof. Jianping Zhang, Prof. Ruimin Han and Prof. Anchi Yu in Department of Chemistry, Renmin

University of China are highly acknowledged for useful suggestions and discussions.

## Notes and references

<sup>a</sup> Department of Chemistry, Renmin University of China, Beijing 100872, P. R. China. E-mail: jinzx@ruc.edu.cn

<sup>b</sup> College of Chemistry and Molecular Engineering, Peking University, Beijing 100871, P. R. China.

<sup>c</sup> Key Laboratory of Analytical Chemistry for Living Biosystems, Institute of Chemistry Chinese Academy of Sciences, Beijing National Laboratory for Molecular Sciences, Beijing 100190, P. R. China.

<sup>d</sup> Beijing Center for Mass Spectrometry, Beijing 100190, P. R. China.

† Electronic Supplementary Information (ESI) available: [supplementary figures and table]. See DOI: 10.1039/b000000x/

- 1 J. H. Waite and M. L. Tanzer, *Science* **1981**, *212*, 1038.
- 2 H. Lee, B. P. Lee and P. B. Messersmith, *Nature* **2007**, *448*, 338.
- 3 H. Lee, N. F. Scherer and P. B. Messersmith, *Proc. Natl. Acad. Sci. U.S.A.* **2006**, *103*, 12999.
- 4 W. Wei, J. Yu, C. Broomell, J. N. Israelachvili and J. H. Waite, *J. Am. Chem. Soc.* **2013**, *135*, 377.
- 5 Q. Ye, F. Zhou and W. M. Liu, *Chem. Soc. Rev.* **2011**, *40*, 4244.

- 6 B. P. Lee, P. B. Messersmith, J. N. Israelachvili and J. H. Waite, *Annu. Rev. Mater. Res.* **2011**, *41*, 99.
- 7 J. Yu, W. Wei, M. S. Menyo, A. Masic, J. H. Waite and J. N. Israelachvili, *Biomacromolecules* **2013**, *14*, 1072.
- 8 B. H. Kim, D. H. Lee, J. Y. Kim, D. O. Shin, H. Y. Jeong, S. Hong, J. M. Yun, C. M. Koo, H. Lee and S. O. Kim, *Adv. Mater.* **2011**, *23*, 5618.
- 9 Z. Y. Xi, Y. Y. Xu, L. P. Zhu, Y. Wang and B. K. Zhu, *J. Membrane Sci.* **2009**, *327*, 244.
- 10 D. R. Dreyer, D. J. Miller, B. D. Freeman, D. R. Paul and C. W. Bielawski, *Chem. Sci.* **2013**, *4*, 3796.
- 11 H. Lee, S. M. Dellatore, W. M. Miller and P. B. Messersmith, *Science* **2007**, *318*, 426.
- 12 M. E. Lyng, R. van der Westen, A. Postma and B. Stadler, *Nanoscale* **2011**, *3*, 4916.
- 13 H. Lee, J. Rho and P. B. Messersmith, *Adv. Mater.* **2009**, *21*, 431.
- 14 N. F. Della Vecchia, R. Avolio, M. Alfe, M. E. Errico, A. Napolitano and M. d'Ischia, *Adv. Funct. Mater.* **2013**, *23*, 1331.
- 15 B. Wang, G. Wang, B. Zhao, J. Chen, X. Zhang and R. Tang, *Chem. Sci.* **2014**, *5*, 3463.
- 16 S. M. Kang, N. S. Hwang, J. Yeom, S. Y. Park, P. B. Messersmith, I. S. Choi, R. Langer, D. G. Anderson and H. Lee, *Adv. Funct. Mater.* **2012**, *22*, 2949.
- 17 E. Ko, K. Yang, J. Shin and S.-W. Cho, *Biomacromolecules* **2013**, *14*, 3202.
- 18 Y. M. Shin, Y. B. Lee, S. J. Kim, J. K. Kang, J.-C. Park, W. Jang and H. Shin, *Biomacromolecules* **2012**, *13*, 2020.
- 19 S. H. Ku, J. S. Lee and C. B. Park, *Langmuir* **2010**, *26*, 15104.
- 20 K. J. Jeong, L. Wang, C. F. Stefanescu, M. W. Lawlor, J. Polat, C. H. Dohlman, R. S. Langer and D. S. Kohane, *Soft Matter* **2011**, *7*, 8305.
- 21 X. Yu, H. L. Fan, L. Wang and Z. X. Jin, *Angew. Chem. Int. Ed.* **2014**, *53*, 12600.
- 22 N. F. Della Vecchia, A. Luchini, A. Napolitano, G. D'Errico, G. Vitiello, N. Szekely, M. d'Ischia and L. Paduano, *Langmuir* **2014**, *30*, 9811.
- 23 N. Farnad, K. Farhadi and N. H. Voelcker, *Water, Air, Soil Pollut.* **2012**, *223*, 3535.
- 24 X. Zhang, S. Wang, L. Xu, L. Feng, Y. Ji, L. Tao, S. Li and Y. Wei, *Nanoscale* **2012**, *4*, 5581.
- 25 K.-Y. Ju, Y. Lee, S. Lee, S. B. Park and J.-K. Lee, *Biomacromolecules* **2011**, *12*, 625.
- 26 Y. Liu and J. D. Simon, *Pigm. Cell Res.* **2003**, *16*, 72.
- 27 M. d'Ischia, A. Napolitano, V. Ball, C.-T. Chen and M. J. Buehler, *Acc. Chem. Res.* **2014**, *47*, 3541.
- 28 M. Arzillo, G. Mangiapia, A. Pezzella, R. K. Heenan, A. Radulescu, L. Paduano, M. d'Ischia, *Biomacromolecules* **2012**, *13*, 2379.
- 29 D.-x. Tan, R. J. Reiter, L. C. Manchester, M. t. Yan, M. El-Sawi, R. M. Sainz, J. C. Mayo, R. Kohen, M. C. Allegra and R. Hardelan, *Curr. Top. Med. Chem. (Sharjah, United Arab Emirates)* **2002**, *2*, 181.
- 30 G. Hervieu, *Expert Opin. Ther. Targets* **2003**, *7*, 495.
- 31 Y. Liu, K. Ai, J. Liu, M. Deng, Y. He and L. Lu, *Adv. Mater.* **2013**, *25*, 1353.
- 32 S. D. Grosse and J. S. Collins, *Birth Defects Res., Part A* **2007**, *79*, 737.
- 33 W. Xia and P. S. Low, *J. Med. Chem.* **2010**, *53*, 6811.
- 34 A. Napolitano, A. Pezzella, G. Prota, R. Seraglia and P. Traldi, *Rapid Commun. Mass Spectrom.* **1996**, *10*, 468.
- 35 C. Kroesche and M. G. Peter, *Tetrahedron* **1996**, *52*, 3947.
- 36 A. Pezzella, A. Napolitano, M. d'Ischia, G. Prota, R. Seraglia and P. Traldi, *Rapid Commun. Mass Spectrom.* **1997**, *11*, 368.
- 37 H. Okuda, K. Yoshino, K. Wakamatsu, S. Ito and T. Sota, *Pigm. Cell Melanoma Res.* **2014**, *27*, 664.
- 38 P. Meredith, B. J. Powell, J. Riesz, S. P. Nighswander-Rempel, M. R. Pederson and E. G. Moore, *Soft Matter* **2006**, *2*, 37.
- 39 P. Meredith and T. Sarna, *Pigm. Cell Res.* **2006**, *19*, 572.
- 40 M. J. Frisch, G. W. Trucks, H. B. Schlegel, G. E. Scuseria, M. A. Robb, J. R. Cheeseman, G. Scalmani, V. Barone, B. Mennucci, G. A. Petersson, H. Nakatsuji, M. Caricato, X. Li, H. P. Hratchian, A. F. Izmaylov, J. Bloino, G. Zheng, J. L. Sonnenberg, M. Hada, M. Ehara, K. Toyota, R. Fukuda, J. Hasegawa, M. Ishida, T. Nakajima, Y. Honda, O. Kitao, H. Nakai, T. Vreven, J. A. Montgomery, Jr., J. E. Peralta, F. Ogliaro, M. Bearpark, J. J. Heyd, E. Brothers, K. N. Kudin, V. N. Staroverov, R. Kobayashi, J. Normand, K. Raghavachari, A. Rendell, J. C. Burant, S. S. Iyengar, J. Tomasi, M. Cossi, N. Rega, J. M. Millam, M. Klene, J. E. Knox, J. B. Cross, V. Bakken, C. Adamo, J. Jaramillo, R. Gomperts, R. E. Stratmann, O. Yazyev, A. J. Austin, R. Cammi, C. Pomelli, J. W. Ochterski, R. L. Martin, K. Morokuma, V. G. Zakrzewski, G. A. Voth, P. Salvador, J. J. Dannenberg, S. Dapprich, A. D. Daniels, O. Farkas, J. B. Foresman, J. V. Ortiz, J. Cioslowski, D. J. Fox, Gaussian, Inc., Revision A.02, Gaussian, Inc., Wallingford CT, 2009.
- 41 J. J. P. Stewart, MOPAC 2012, Stewart Computational Chemistry, Version 14.247W web: [HTTP://OpenMOPAC.net](http://OpenMOPAC.net)
- 42 J. D. C. Maia, G. A. U. Carvalho, C. P. Manguiera, Jr., S. R. Santana, L. A. F. Cabral, G. B. Rocha, *J. Chem. Theory Comput.* **2012**, *8*, 3072.
- 43 F. Bernsmann, V. Ball, F. Addiego, A. Ponche, M. Michel, J. J. de Almeida Gracio, V. Toniazzo and D. Ruch, *Langmuir* **2011**, *27*, 2819.
- 44 S. Reale, M. Crucianelli, A. Pezzella, M. d'Ischia and F. De Angelis, *J. Mass Spectrom.* **2012**, *47*, 49.
- 45 E. Kaxiras, A. Tsolakidis, G. Zonios and S. Meng, *Phys. Rev. Lett.* **2006**, *97*, 218102.
- 46 S. Meng and E. Kaxiras, *Biophys. J.* **2008**, *94*, 2095.
- 47 J. Liebscher, R. Mrowczynski, H. A. Scheidt, C. Filip, N. D. Hadade, R. Turcu, A. Bende and S. Beck, *Langmuir* **2013**, *29*, 10539.
- 48 S. Choi, Ph.D Thesis, University of Houston, Houston, TX, 1977.
- 49 D. R. Dreyer, D. J. Miller, B. D. Freeman, D. R. Paul and C. W. Bielawski, *Langmuir* **2012**, *28*, 6428.
- 50 C.-T. Chen, V. Ball, J. J. de Almeida Gracio, M. K. Singh, V. Toniazzo, D. Ruch and M. J. Buehler, *ACS Nano* **2013**, *7*, 1524.
- 51 X. Yu, H. L. Fan, Y. Liu, Z. J. Shi and Z. X. Jin, *Langmuir* **2014**, *30*, 5497.
- 52 W. Qiang, W. Li, X. Li, X. Chen and D. Xu, *Chem. Sci.* **2014**, *5*, 3018.
- 53 J. D. Simon, *Acc. Chem. Res.* **2000**, *33*, 307.
- 54 L. Panzella, G. Gentile, G. D'Errico, N. F. Della Vecchia, M. E. Errico, A. Napolitano, C. Carfagna and M. d'Ischia, *Angew. Chem. Int. Ed.* **2013**, *125*, 1291